

Higher Control Scheme Using Neural Second Order Sliding Mode and ANFIS-SVM strategy for a DFIG-Based Wind Turbine

Habib Benbouhenni¹, Zinelaabidine Boudjema², Abdelkader Belaidi¹

Abstract— In this paper, we propose an advanced control scheme using neural second order sliding mode (NSOSMC) and adaptive neuro-fuzzy inference system space vector modulation (ANFIS-SVM) strategy for a doubly fed induction generator (DFIG) integrated into a wind turbine system (WTS). The used hybrid control system composed of artificial intelligence techniques and second-order sliding mode applied to ensure better powers performances provided by the WTS. The obtained simulation results showed that the proposed control structure has active and reactive powers with low ripples and low stator current harmonic distortion.

Keywords— DFIG, WTS, NSOSMC, ANFIS-SVM.

I. INTRODUCTION

Doubly fed induction generator wind turbines with converters rated at about 25-30% of the generator rating are becoming increasingly popular [1]. Control and operation of DFIG have been the subject of intense research during the last few years [2]. However, the stator of the DFIG is connected to the energy grid and the rotor is connected to AC-DC-AC converter [3]. Various strategies have been proposed for studying the behaviour of DFIG based WTS during ordinary operation [4].

In the control system, the indirect vector control (IVC) using proportional-integral (PI) regulators is a traditional strategy used to control DFIG-based WTSS. However, PI regulator performance is highly dependant on the tuning of parameters and accurate tracking of angular information of stator flux voltage. In [5], the IVC strategy gives more harmonic distortion of rotor current and power ripples of DFIG-based WTSS.

For high performance and robust control of DFIG, a sliding mode controller (SMC) was studied in the literature [6-9]. It is a high frequency switching control strategy for nonlinear systems with uncertainties. It can offer much good performances against unmodeled dynamics, insensitivity to

parameters variation, and fast dynamic response. Fuzzy logic controller (FLC) and SMC technique are combined to control DFIG [10].

Since the pulse width modulation (PWM) strategy is widely used in control of the AC machine, especially for scalar control where the stator voltage and frequency can be controlled with the minimum online computational requirement. The PWM technique is simple and easy to implement. However, this method gives more total harmonic distortion (THD). On the other hand, the SVM strategy gives 15 % more voltage output compare to the PWM strategy and minimizes the THD value of stator current.

Since the SVM strategy of electrical drives has become an attracting topic in research and academic community over the past decade. Nevertheless, this type of control has essential disadvantages and advantages. The basic disadvantages of the SVM strategy are the current ripple. In the aim to improve the performance of the electrical drives based on SVM, adaptive neuro-fuzzy inference system SVM (ANFIS-SVM) strategy is proposed in this work.

In [11], the author proposed a new SVM strategy based on calculating of maximum and minimum of three-phase voltages. Fuzzy logic (FL) and two-level SVM strategy are combined to control the DFIG [12]. In [13], the authors proposed a three-level FSVM technique to minimize the harmonic distortion of stator current. In [14], an reactive and stator active power proportional-integral controllers and four-level FSVM were combined to reduces the electromagnetic torque ripples, active and reactive power ripples. In [15], a modified SVM technique was proposed based on artificial neural networks (ANNs) control to regulate the torque and active power of the DFIG.

In this article, two different techniques of a DFIG will be simulated and compared with each other; conventional IVC with PWM strategy (IVC-PWM) and NSOSMC with ANFIS-SVM strategy (NSOSMC-ANFIS-SVM). The advantages of the proposed technique will be tinted by studying the effect of ripples performance.

II. WIND TURBINE

The input power of the wind turbine is [16, 17]:

$$P_v = 0.5\rho S_w v^3 \quad (1)$$

Where ρ is air density, S_w is wind turbine blades swept area in the wind, v is wind speed.

The output power of wind turbine is:

$$P_m = C_p \cdot P_v \quad (2)$$

Manuscript received September 6, 2018, revised March 25, 2019, revised June 5, 2019.

Habib Benbouhenni is with the Electrical Engineering Department, National Polytechnique School of Oran Maurice Audin, Bp.1523 El M'Naouer 31000 Oran, Algeria (corresponding author to provide phone: +213663956329; e-mail: habib0264@gmail.com).

Zinelaabidine Boudjema is with Electrical Engineering Department, Hassiba Benbouali University, LGEER Research Laboratory, Hay Salem 02000 Chlef, Algeria. (e-mail: boudjemaa1983@yahoo.fr).

Abdelkader Belaidi is with the Electrical Engineering Department, National Polytechnique School of Oran Maurice Audin, Bp.1523 El M'Naouer 31000 Oran, Algeria (e-mail: belaidiaek@gmail.com).

C_p can be described as:

$$C_p(\beta, \lambda) = C_1 \left(\frac{C_2}{\lambda_i} - C_3 \beta - C_4 \right) \exp\left(\frac{-C_5}{\lambda_i}\right) + C_6 \lambda \quad (3)$$

$$\lambda = \frac{R \cdot \Omega_t}{v} \quad (4)$$

where C_p is the wind turbine power conversion efficiency. λ is the tip speed ratio. β is the blade pitch angle in a pitch-controlled wind turbine. R is blade radius. Ω is angular speed of the turbine.

$$\frac{1}{\lambda_i} = \frac{1}{\lambda + 0.08\beta} - \frac{0.035}{\beta^3 + 1} \quad (5)$$

where, $C_1=0.5176$, $C_2=116$, $C_3=0.4$, $C_4=5$, $C_5=21$, $C_6=0.0068$.

The torque produced by the turbine is expressed in the following way:

$$T_t = \frac{P_t}{\Omega_t} = 0.5 \rho \cdot \pi \cdot R^3 \cdot v^2 \cdot C_t \quad (6)$$

where, C_t is the torque coefficient expressed by:

$$C_t = \frac{C_p}{\lambda} \quad (7)$$

III. MODEL OF DFIG

The traditional equations of flux and voltages for the DFIG in a d - q synchronously rotating reference frame can be written as follows [18, 19].

$$\begin{cases} V_{ds} = R_s I_{ds} + \frac{d}{dt} \psi_{ds} - \omega_s \psi_{qs} \\ V_{qs} = R_s I_{qs} + \frac{d}{dt} \psi_{qs} + \omega_s \psi_{ds} \\ V_{dr} = R_r I_{dr} + \frac{d}{dt} \psi_{dr} - \omega_r \psi_{qr} \\ V_{qr} = R_r I_{qr} + \frac{d}{dt} \psi_{qr} + \omega_r \psi_{dr} \end{cases} \quad (8)$$

where: I_{dr} and I_{qr} are the rotor currents

I_{ds} and I_{qs} are the stator currents

V_{ds} and V_{qs} are the stator Voltages

V_{dr} and V_{qr} are the rotor voltages

R_r is the rotor resistance

R_s is the stator resistance

$$\begin{cases} \psi_{ds} = L_s I_{ds} + M I_{dr} \\ \psi_{qs} = L_s I_{qs} + M I_{qr} \\ \psi_{dr} = L_r I_{dr} + M I_{ds} \\ \psi_{qr} = L_r I_{qr} + M I_{qs} \end{cases} \quad (9)$$

where: L_r is the inductance of the rotor

L_s is the inductance of the stator

M is the mutual inductance

Ψ_{dr} and Ψ_{qr} is the rotor fluxes

Ψ_{qs} and Ψ_{ds} is the stator fluxes.

The rotor and stator angular velocities are linked by the following relation:

$$\omega_s - \omega = \omega_r \quad (10)$$

ω : is the mechanical pulsation of the DFIG

ω_s : is the electrical pulsation of the stator. ω_r is the rotor one.

The electrical model of the DFIG is completed by the following mechanical equation:

$$T_e - T_r = J \cdot \frac{d\Omega}{dt} + f \cdot \Omega \quad (11)$$

The torque can be written as follows:

$$T_e = \frac{3}{2} p \frac{M}{L_s} (I_{dr} \psi_{qs} - I_{qr} \psi_{ds}) \quad (12)$$

T_r is the load torque, Ω is the mechanical rotor speed, J is the inertia, f is the viscous friction coefficient, and p is the number of pole pairs.

The stator side reactive and active powers are defined as:

$$\begin{cases} P_s = \frac{3}{2} (V_{ds} I_{ds} + V_{qs} I_{qs}) \\ Q_s = \frac{3}{2} (V_{qs} I_{ds} - V_{ds} I_{qs}) \end{cases} \quad (13)$$

where: P_s is the stator active power

Q_s is the stator reactive power.

IV. INDIRECT VECTOR CONTROL

In this section, we use a Park reference frame linked to the stator flux (Fig. 1). The detailed indirect vector control (IVC) of the DFIG has been studied in the literature [20-22].

The control stator active power and reactive power of the DFIG directly connected through the stator windings to the grid, is shown in Fig. 2. Therefore, we control the reactive and active powers axis separately by adding PI controllers in each loop. A control block diagram is shown in Fig. 3. In [23], a IVC strategy with two-level FSVN technique was proposed to regulate stator reactive power and electromagnetic torque.

$$\psi_{qs} = 0, \psi_{ds} = \psi_s \quad (14)$$

$$\begin{cases} V_{qs} = 0 \\ V_{ds} = \omega_s \psi_s \end{cases} \quad (15)$$

$$\begin{cases} I_{ds} = -\frac{M}{L_s} I_{dr} + \frac{\psi_s}{L_s} \\ I_{qs} = -\frac{M}{L_s} I_{qr} \end{cases} \quad (16)$$

The expression of the rotor voltages becomes:

$$\begin{cases} V_{dr} = R_r \cdot I_{dr} - \omega_r \cdot \left(L_r - \frac{M^2}{L_s} \right) \cdot I_{qr} \\ V_{qr} = R_r \cdot I_{qr} + \omega_r \cdot \left(L_r - \frac{M^2}{L_s} \right) \cdot I_{dr} + g \cdot \frac{M \cdot V_s}{L_s} \end{cases} \quad (17)$$

The expression of the rotor fluxes and powers becomes:

V. ANFIS-SVM STRATEGY

This paper presents a new technique of two-level SVM using adaptive network-based fuzzy inference system (ANFIS) control (2L-ANFIS-SVM). This proposed technique is simple and easy to implement [24, 25]. However, the ANFIS controller is the combination of neural networks and fuzzy logic. This hybrid combination enables to minimize the complexity of power intelligent system. The ANFIS controller was developed in the early 1990s. The advantages of the ANFIS controller is not needed to mathematical model of system and easy to implement. Since the SVM technique is not based on separate calculations for each arm of the inverter, but the determination of a global control vector approximated in an over modulation techniques. Like every control technique has some advantages and disadvantages.

The advantages of the traditional SVM technique are presented in [26]. On the other hand, this strategy is difficult to implement compared to traditional PWM strategy. A new SVM technique for a two-level inverter is proposed in [12, 23]. This new SVM strategy based on calculation of maximum and minimum of three-phase voltages (V_a, V_b, V_c). The block diagram of the proposed SVM strategy for the two-level inverter is as shown in Fig. 4. Fig. 5 represents the block diagram of the hysteresis comparators for the two-level inverter. The $F_1(u), F_2(u)$ and $F_3(u)$ is given by:

$$\begin{cases} F_1(u) = (E/3)(2 * u(1) - u(2) - u(3)) \\ F_2(u) = (E/3)(-u(1) + 2 * u(2) - u(3)) \\ F_3(u) = (E/3)(-u(1) - u(2) + 2 * u(3)) \end{cases} \quad (20)$$

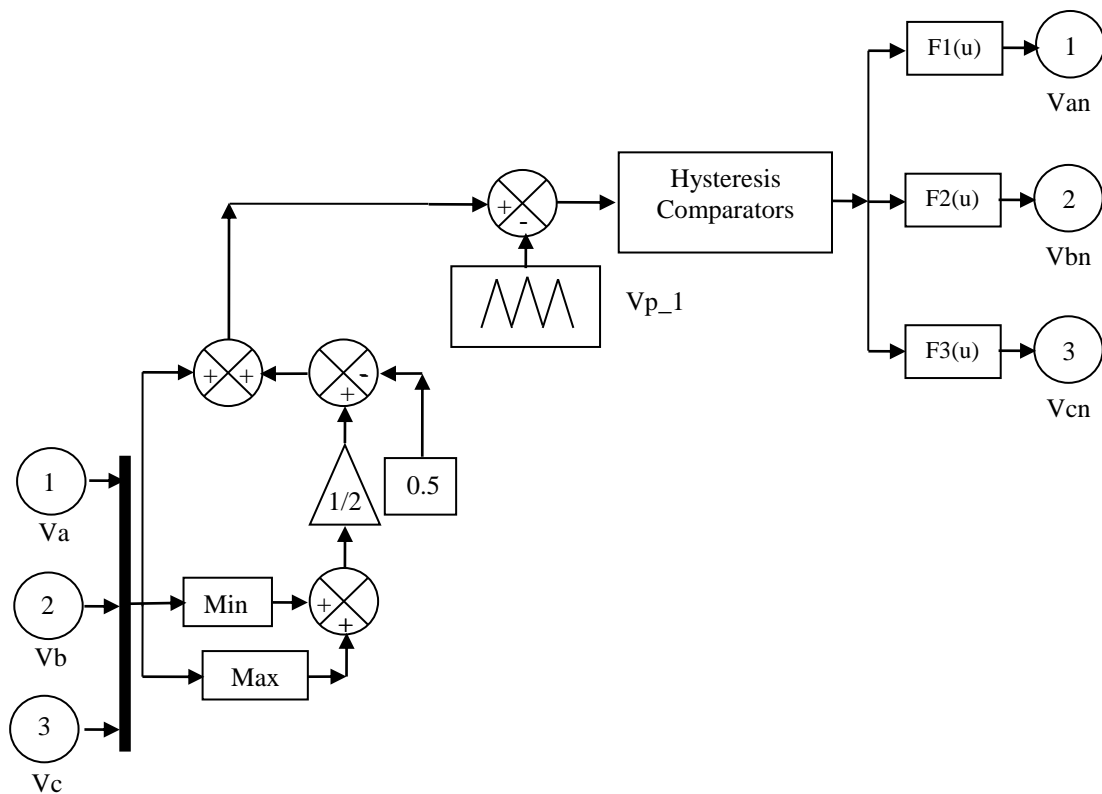


Fig. 4 Simulation block of the proposed SVM technique.

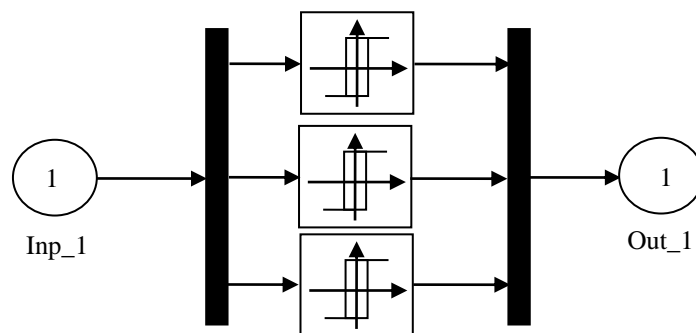


Fig. 5 Block diagram of the hysteresis comparators.

Two parameters characterized the proposed SVM technique:

- The index of modulation (m): defined by the ratio of the carrying and reference wave frequencies.
- The modulation factor (r): the amplitude ration.

The principle of the ANFIS-SVM strategy is similar to 2L-SVM technique. However, the hysteresis controllers are replaced by ANFIS controllers and this proposed technique has the advantage of simplicity and easy implementation.

On the other hand, the ANFIS-SVM strategy gives more minimum harmonic distortion of stator current compared to conventional SVM strategy.

This strategy reduces the ripple of electromagnetic torque, stator reactive and active power. The structure of SVM based on ANFIS controllers is shown in Fig. 6. Fig. 7 represents the block diagram of the ANFIS hysteresis comparators for two-level ANFIS-SVM strategy. The block diagram of ANFIS controllers based hysteresis comparators is shown in Fig. 8.

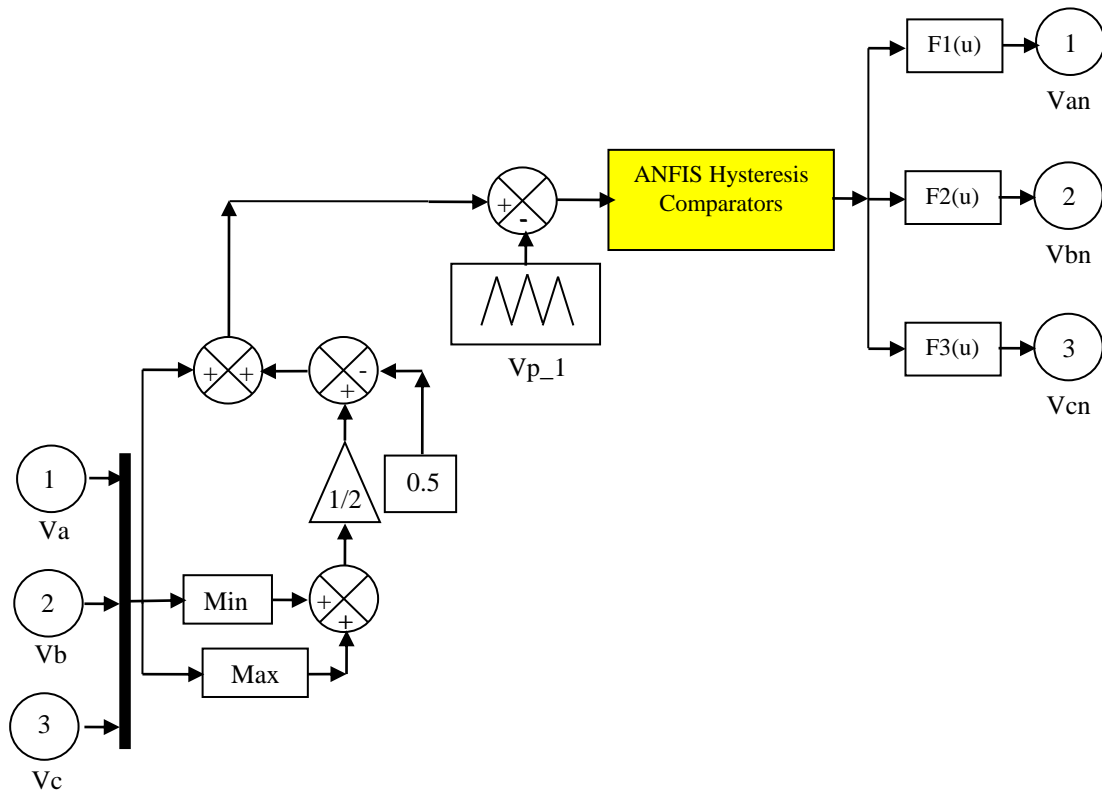


Fig. 6 Simulation block of the proposed ANFIS-SVM technique.

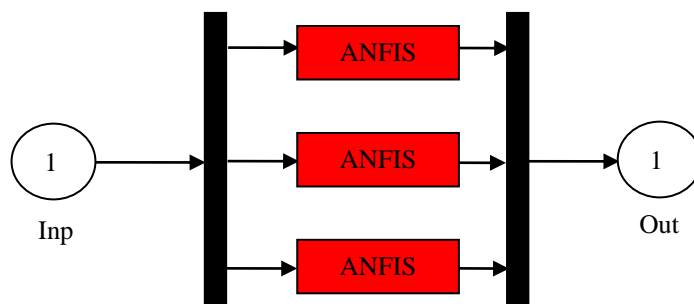


Fig. 7 Block diagram of the ANFIS hysteresis comparators.

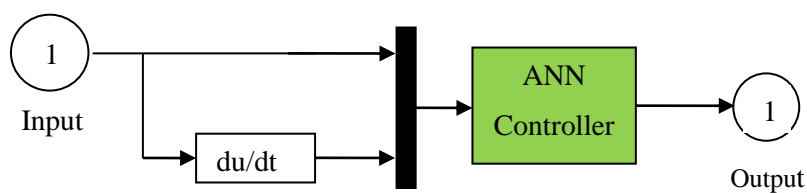


Fig. 8 Architecture of ANFIS controller.

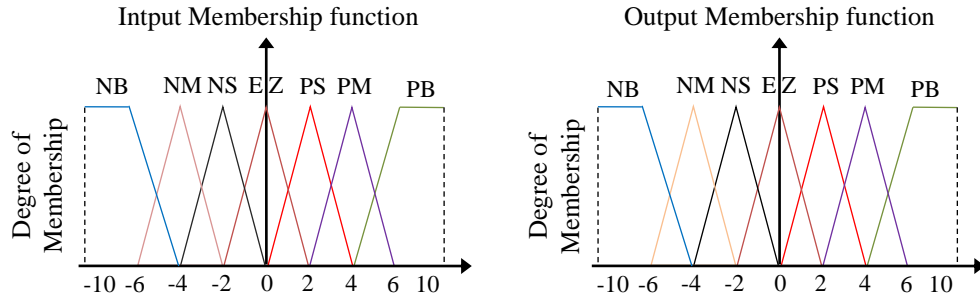


Fig. 9 Fuzzy sets and its memberships functions.

The membership function definition for the input variables and output variables is given by Fig. 9.

The FLC rules for the proposed system are given in Table I [27, 28]. Table II shows the parameters of FLC controller.

TABLE I THE FLC RULES

e	NB	NM	NS	EZ	PS	PM	PB
Δe							
NB	NB	NB	NB	NB	NM	NS	EZ
NM	NB	NB	NB	NM	NS	EZ	PS
NS	NB	NB	NM	NS	EZ	PS	PM
EZ	NB	NM	NS	EZ	PS	PM	PB
PS	NM	NS	EZ	PS	PM	PB	PB
PM	NS	EZ	PS	PM	PB	PB	PB
PB	EZ	PS	PM	PB	PB	PB	PB

TABLE II PARAMETERS OF FLC CONTROLLER

Fis type	Mamdani
And method	Min
Or method	Max
Implication	Min
Aggregation	Max
Defuzzification	Centroid

The training used is that of the algorithm, Gradient descent with momentum & Adaptive LR. The convergence of the network in summer obtained by using the value of the parameters grouped in Table III.

TABLE III PARAMETERS OF THE ALR ALGORITHM

Parameters of the ALR	Values
Number of hidden layer	8
TrainParam.Lr	0.002
TrainParam.show	50
TrainParam.epochs	300
Coeff of acceleration of convergence (mc)	0.9
TrainParam.goal	0
TrainParam.mu	0.9
Functions of activation	Tensing, Purling, gensim

VI. NEURO-SECOND ORDER SLIDING MODE CONTROLLER

A. Second-order Sliding Mode Controller

The basic idea of the SMC is detailed in [29, 30]. The SMC method is developed from variable structure control to solve the disadvantage of other designs of nonlinear control systems. However, the design of SMC strategy supports the desired stability problems and performance in a systematic way [31]. The following three steps are necessary for the implementation of the SMC technique:

- The choice of the surface,

- The convergence condition,
- Calculation of the control law.

In this paper, we use the SOSMC strategy applied to the DFIG machine. The advantage of the SOSMC is reducing chattering nonlinearities, and robustness. We choose the error between the reference stator energies and measured as second-order sliding mode surfaces, so we can write the following expression:

$$\begin{bmatrix} S_p \\ S_q \end{bmatrix} = \begin{bmatrix} P_{sref} - P_s \\ Q_{sref} - Q_s \end{bmatrix} \quad (21)$$

We derived the above errors, we obtain

$$\begin{bmatrix} \dot{S}_p \\ \dot{S}_q \end{bmatrix} = \begin{bmatrix} \dot{P}_{sref} - P_s \\ \dot{Q}_{sref} - Q_s \end{bmatrix} \quad (22)$$

Then we will have

$$\begin{bmatrix} \dot{S}_p \\ \dot{S}_q \end{bmatrix} = \begin{bmatrix} \dot{P}_{sref} - \frac{\alpha}{\sigma L_r} \left[V_{qr} - R_r I_{qr} - g.w_s \sigma L_r I_{dr} - g \frac{M.V_s}{L_s} \right] \\ \dot{Q}_{sref} - \frac{\alpha}{\sigma L_r} \left[V_{dr} - R_r I_{dr} + g.w_s \sigma L_r I_{qr} \right] \end{bmatrix} \quad (23)$$

where: $\alpha = -V_s M/L_s$

If we define the A1 and A2 functions as follows.

$$\begin{bmatrix} A_1 \\ A_2 \end{bmatrix} = \begin{bmatrix} \dot{P}_{sref} - \frac{\alpha}{\sigma L_r} \left[-R_r I_{qr} - g.w_s \sigma L_r I_{dr} - g \frac{M.V_s}{L_s} \right] \\ \dot{Q}_{sref} - \frac{\alpha}{\sigma L_r} \left[-R_r I_{dr} - g.w_s \sigma L_r I_{qr} \right] \end{bmatrix} \quad (24)$$

Thus we have

$$\begin{bmatrix} \dot{S}_p \\ \dot{S}_q \end{bmatrix} = \begin{bmatrix} \frac{\alpha}{\sigma L_r} V_{qr} + A_1 \\ \frac{\alpha}{\sigma L_r} V_{dr} + A_2 \end{bmatrix} \quad (25)$$

On driving the relationship of equation (25) yields:

$$\begin{bmatrix} \ddot{S}_p \\ \ddot{S}_q \end{bmatrix} = \begin{bmatrix} \frac{\alpha}{\sigma L_r} \dot{V}_{qr} + \dot{A}_1 \\ \frac{\alpha}{\sigma L_r} \dot{V}_{dr} + \dot{A}_2 \end{bmatrix} \quad (26)$$

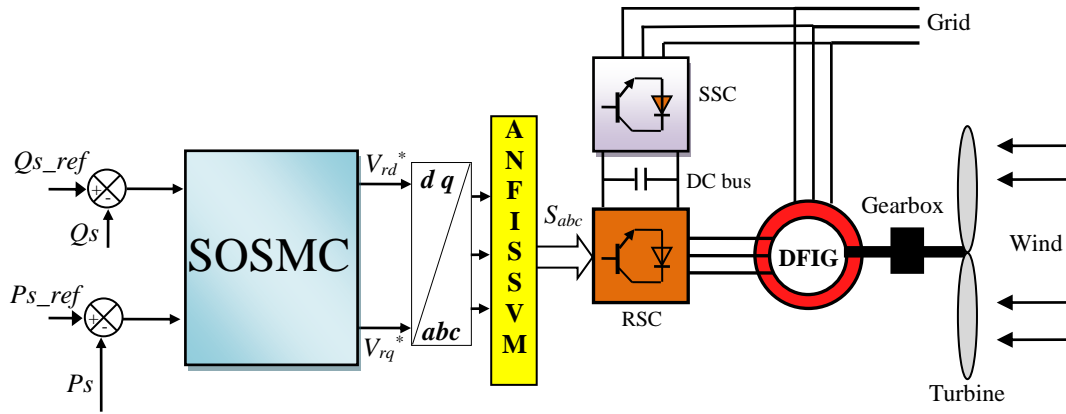


Fig. 10 7SOSMC with ANFIS-SVM strategy of DFIG.

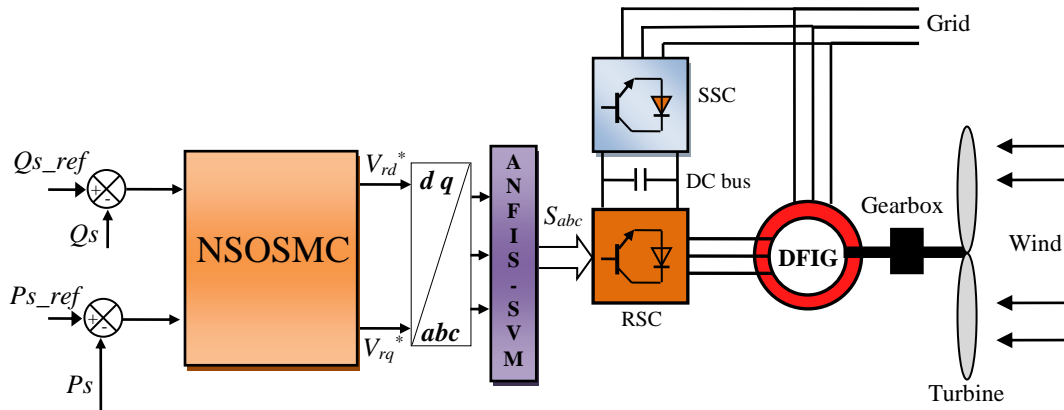


Fig. 11 7NSOSMC with ANFIS-SVM strategy of DFIG.

The SOSMC proposed based on the super twisting algorithm known (ST) which is introduced by Levant.

$$V_{dr} = u_1 + u_2 \quad (27)$$

Then it follows that:

$$\begin{bmatrix} u_1 \\ u_2 \end{bmatrix} = \begin{bmatrix} -\lambda_1 \text{sign}(S_q) \\ -\delta_1 |S_q|^{0.5} \text{sign}(S_q) \end{bmatrix} \quad (28)$$

A. Neuro-second Order Sliding Mode Controller

Artificial neural network (ANN) is an interconnected group of artificial neurones [31]. The application of ANN attracts the attention of many scientists from all over the world [32]. This intelligent technique has many advantages, it is simple architecture, inexact input data, the possibility of approximating non-linear function, insensitivity to the distortion of the network, easy of training and generalization [33, 34].

And:

$$V_{qr} = w_1 + w_2 \quad (29)$$

Including:

$$\begin{bmatrix} w_1 \\ w_2 \end{bmatrix} = \begin{bmatrix} -\lambda_2 \text{sign}(S_p) \\ -\delta_2 |S_p|^{0.5} \text{sign}(S_p) \end{bmatrix} \quad (30)$$

To ensure the convergence of regulators in the infinity of time constants and are chosen to satisfy the following inequality:

$$\begin{cases} \lambda_i \leq \frac{\mu_i}{\sigma \cdot L_r} \\ \delta_i \geq \frac{4\mu_i(\lambda_i + \mu_i)}{(\lambda_i - \mu_i)(L_r \sigma)^2} \\ |A_i| < \mu_i; i=1,2 \end{cases} \quad (31)$$

The SOSMC control of a DFIG based on SVM inverter is shown in Fig. 10.

In this section, we use the Gradient Descent with Momentum & Adaptive LR. This algorithm is a network training function that updates weight and bias values according to gradient descent momentum and an adaptive learning rate. In order to eliminate the chattering phenomenon and improve the SOSMC, we propose to use NSOSMC control. The NSOSMC control of a DFIG based on NSVM inverter is shown in Fig. 11.

The NSOSMC control is a modification of the SOSMC, where the switching controller term $\text{sign}(S(x))$, has been replaced by a neural technique control input as given by Fig. 12 [35].

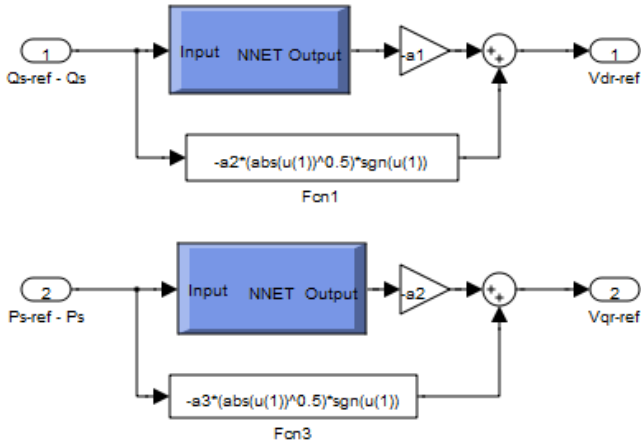


Fig. 12 Block diagram of NSOSMC strategy.

Since, the neural network contains three layers: output layer, input layer and hidden layers. The structure of the proposed neural controllers was a network with one linear input node, 8 neurons in the hidden layer, and one neuron in the output layers.

Fig. 13 shows the neural network training performance of the neural controller for reactive and active powers. Fig. 14 shows the internal structure of the neural controller for reactive and active powers. Fig. 15 block diagram of the internal structure of the hidden layer.

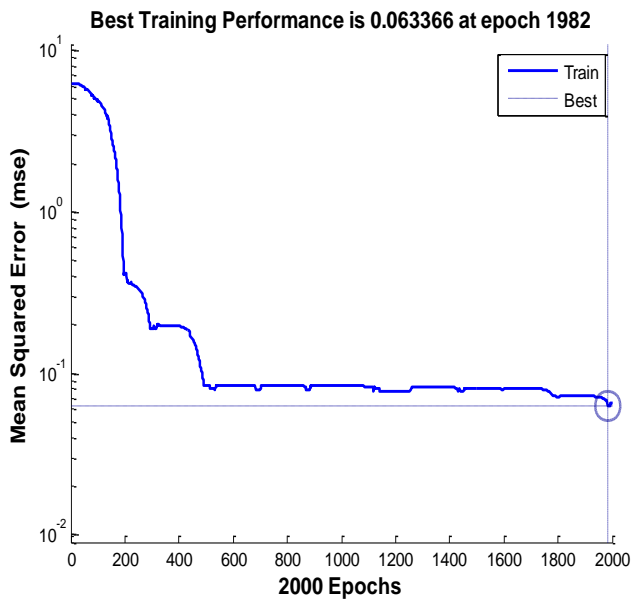


Fig. 13 Neural network training performance.

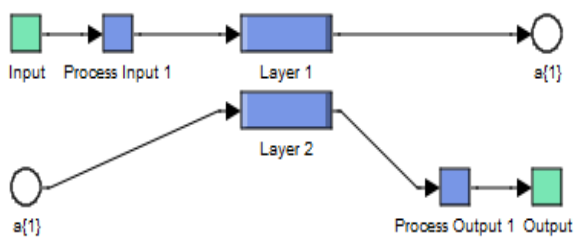


Fig. 14 The internal structure of neural controllers.

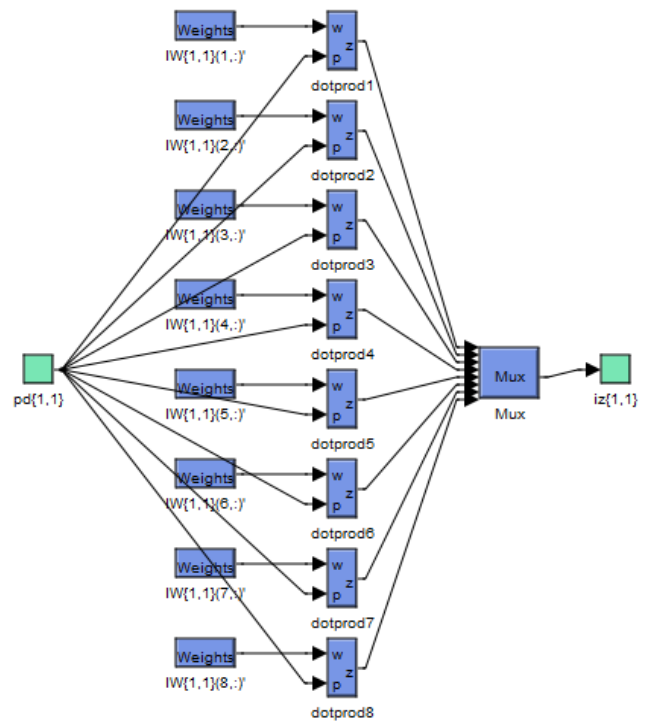


Fig. 15 Block diagram of the internal structure of hidden layer.

VII. SIMULATION RESULTS

In this section, simulations are carried out with a 1.5MW DFIG machine attached to a 398V/50Hz grid, using the Matlab/Simulink software. Parameters of the DFIG are given in Table IV. Two control strategies, IVC-PWM and NSOSMC-ANFIS-SVM control, are simulated and compared regarding reference tracking, stator current harmonics distortion, powers ripples, and robustness against DFIG parameter variations.

TABLE IV THE DFIG PARAMETERS

Parameters	Rated Value	Unity
Nominal power	1.5	MW
Stator voltage	398	V
Stator frequency	50	Hz
Number of pairs poles	2	
Stator resistance	0.012	Ω
Rotor resistance	0.021	Ω
Stator inductance	0.0137	H
Rotor inductance	0.0136	H
Mutual inductance	0.0135	H
Inertia	1000	Kg m ²
Viscous friction	0.0024	Nm/s

A. Reference Tracking Test(RTT)

The objective of this test is the study of the two proposed controls behaviour in reference tracking. The simulation results are presented in Figs. 16-21. As it's shown by Figs. 16-17, for the two proposed strategies, the reactive and active powers track almost perfectly their references values but with important response time for the IVC-PWM control. On the other hand, Figs. 19-20 show the harmonic spectrums of stator current of the DFIG obtained using Fast Fourier Transform (FFT) method for both techniques. It can

be clearly observed that the THD value is reduced for NSOSMC-ANFIS-SVM control. Table V shows the comparative analysis of the THD values of stator current.

TABLE V COMPARATIVE ANALYSIS OF THE THD (RTT)

	THD (%)	
	IVC-PWM	NSOSMC-ANFIS-SVM
Stator current	0.84	0.13

Figs. 22-24 show the zoom in the active power, reactive power and stator current of the IVC-PWM and NSOSMC-ANFIS-SVM strategies. This figure shows that the ripple of active and reactive powers for the NSOSMC-ANFIS-SVM control scheme has almost equal to zero. Therefore it can be considered that the two proposed strategies have a very good performance for this test.

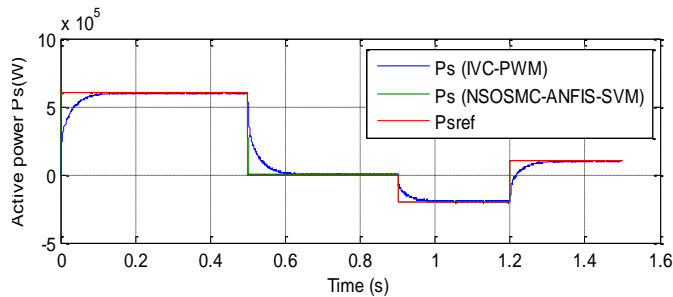


Fig. 16 Active power (RTT).

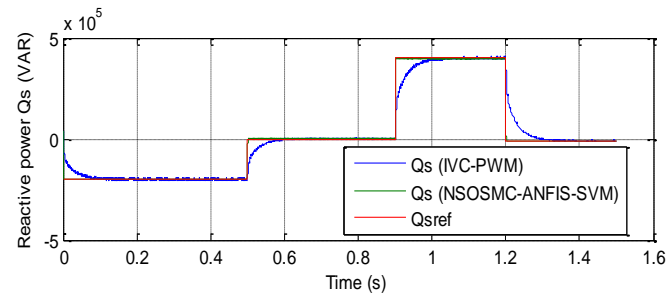


Fig. 17 Reactive power (RTT).

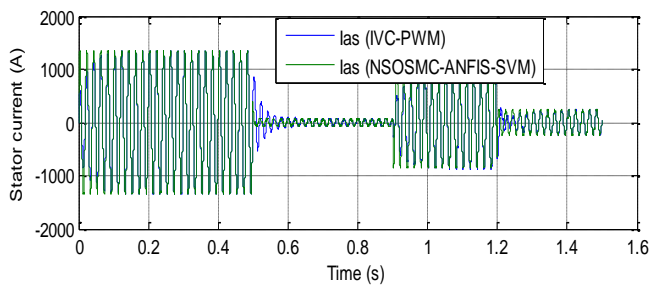


Fig. 18 Stator current (RTT).

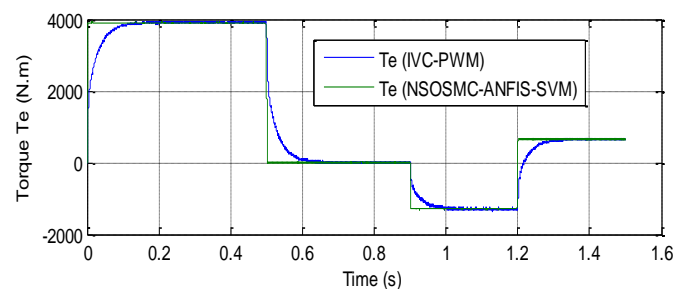


Fig. 19 Electromagnetic torque (RTT).

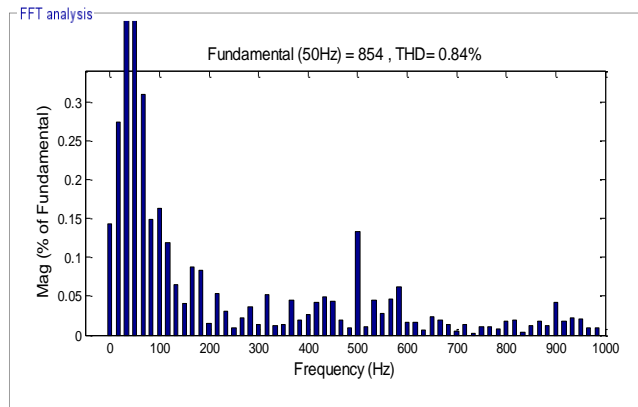
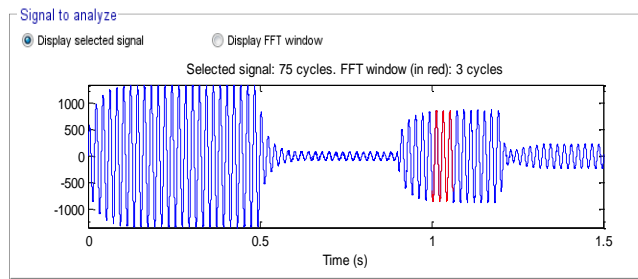


Fig. 20 THD of stator current for the IVC-PWM control (RTT).

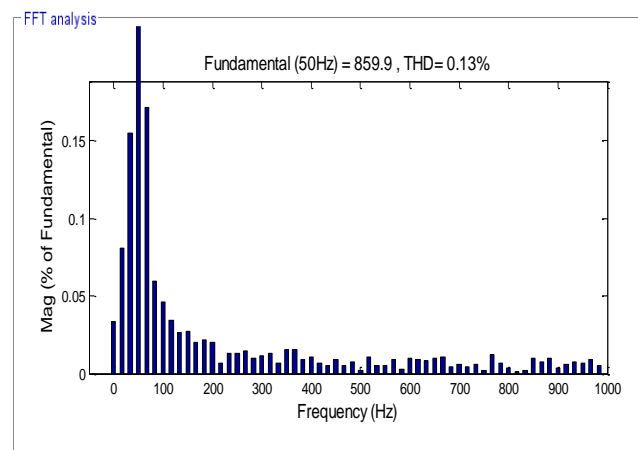
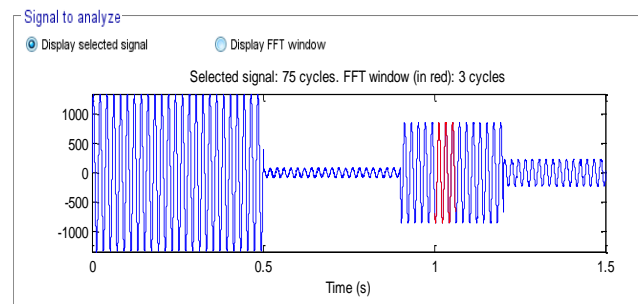


Fig. 21 THD of stator current for the NSOSMC-ANFIS-SVM control (RTT).

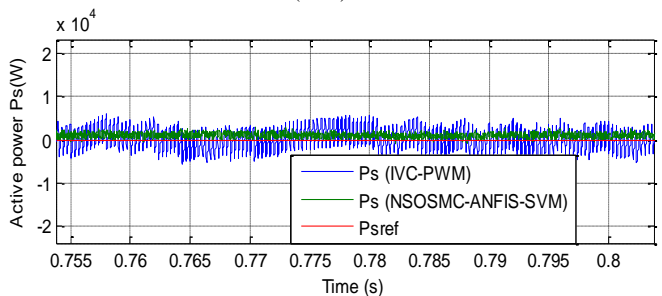


Fig. 22 Zoom in the active power (RTT).

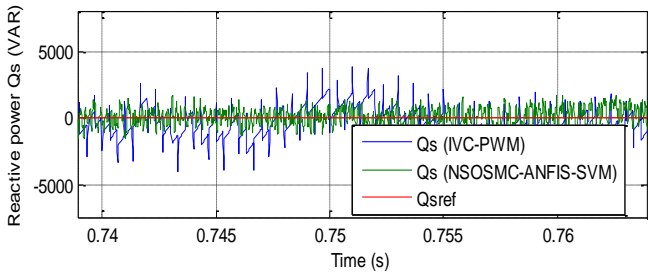


Fig. 23 Zoom in the reactive power (RTT).

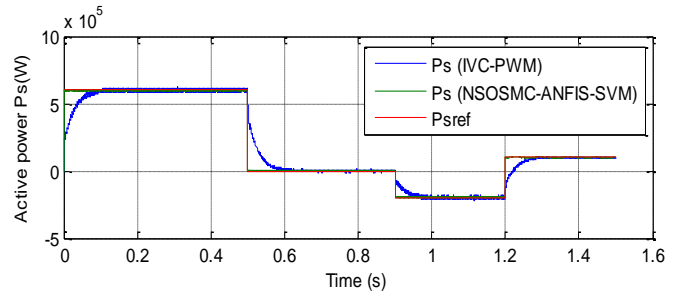


Fig. 26 Active power (RT).

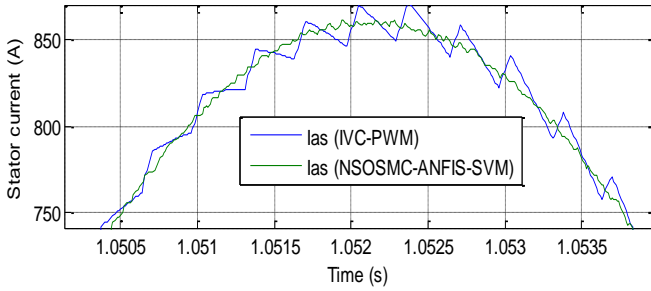


Fig. 24 Zoom in the stator current (RTT).

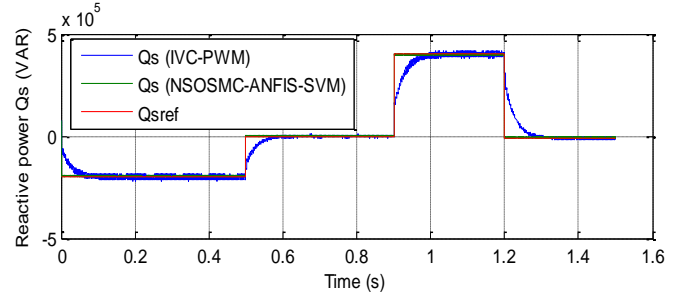


Fig. 27 Reactive power (RT).

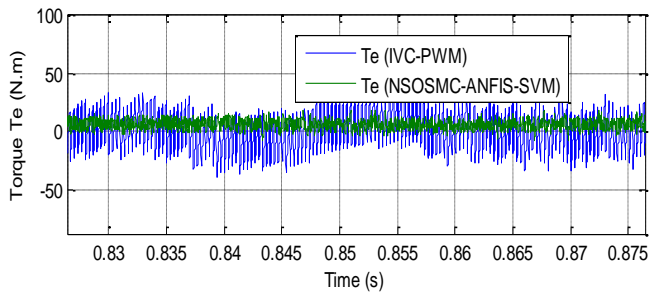


Fig. 25 Zoom in the electromagnetic torque (RTT).

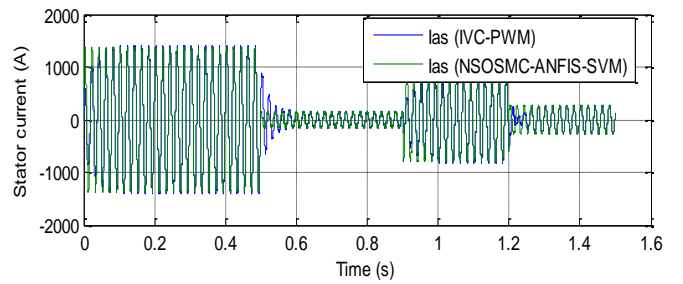


Fig. 28 Stator current (RT).

B. Robustness Test(RT)

In order to test the robustness of the proposed techniques, the DFIG parameters have been intentionally changed such as the values of the resistances R_s and R_r are multiplied by 2 and the values of the inductances L_s and L_r are divided by 2. Simulation results are presented in Figs. 26-30. As it's shown by these figures, these variations present a clear effect on active power, reactive power and stator current curves and that the effect appears more important for the IVC-PWM than that with NSOSMC-ANFIS-SVM control. On the other hand, these results show that the THD value of stator current in the NSOSMC-ANFIS-SVM control scheme has been reduced significantly. Table VI shows the comparative analysis of THD values. Thus, it can be concluded that the proposed NSOSMC-ANFIS-SVM control scheme is more robust than the IVC-PWM one.

TABLE VI COMPARATIVE ANALYSIS OF THE THD (RT)

	THD (%)	
	IVC-PWM	NSOSMC-ANFIS-SVM
Stator current	1.45	0.18

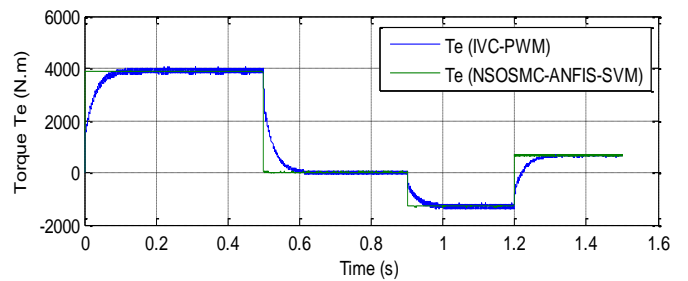


Fig. 29 Electromagnetic torque (RT).

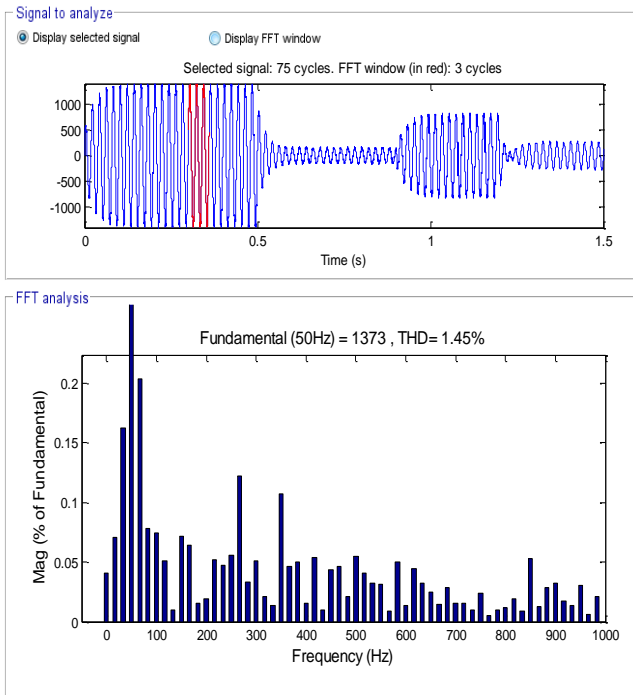


Fig. 30 THD of stator current for the IVC-PWM control (RT).

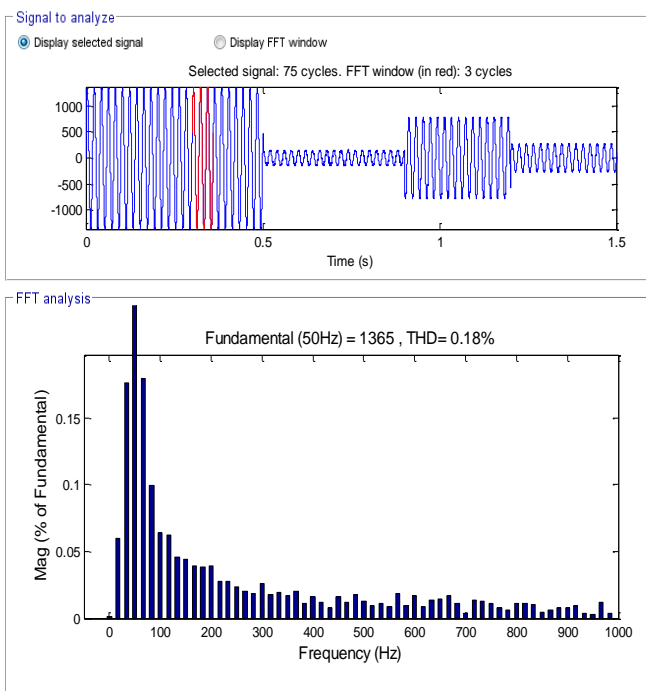


Fig. 31 THD of stator current for the NSOSMC-ANFIS-SVM control (RT).

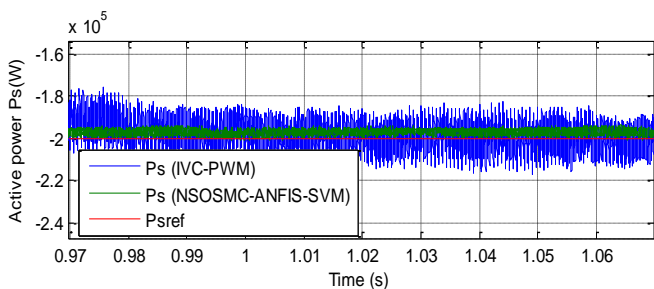


Fig. 32 Zoom in the active power (RT).

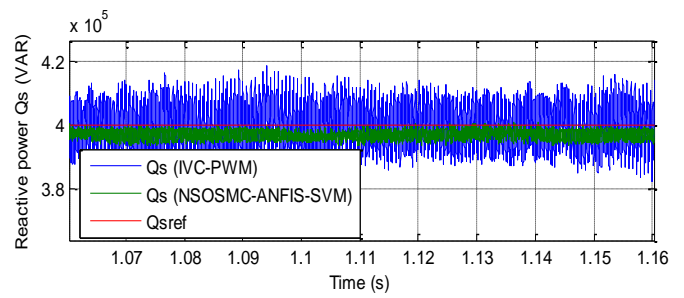


Fig. 33 Zoom in the reactive power (RT).

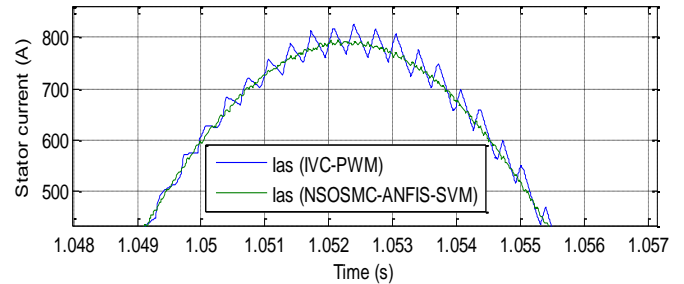


Fig. 34 Zoom in the stator current (RT).

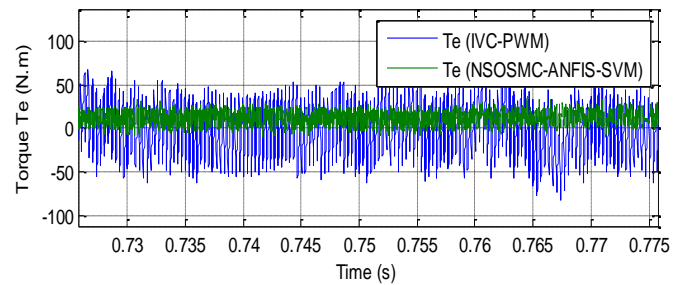


Fig. 35 Zoom in the electromagnetic torque (RT).

VIII. CONCLUSION

A novel robust strategy based on variable structure method of a DFIG has been presented in this article. The DFIG connected directly to the grid by the stator and fed by an ANFIS-SVM strategy on the rotor side. Our objective was the simulation of a neural second order sliding mode control technique with ANFIS-SVM technique of stator active and stator reactive powers generated by the stator side of the DFIG in order to ensure high performances of the DFIG machine and make the system insensible with the external disturbances and the parametric variations. Simulation results have confirmed that the proposed NSOSMC-ANFIS-SVM operates with a very lower ripples power and reduced of the THD value of stator current in term of tracking and robustness test. Basing on all these results it can be concluded that robust strategy as NSOSMC-ANFIS-SVM can be a very good-looking result for the strategy using DFIG such as wind energy transfer systems.

REFERENCES

- [1] A. Boulahia, M. Adel, B. Hocine, Predictive power control of grid and rotor side converters in doubly fed induction generators based wind turbine, *International Journal of Electrical and Computer Engineering*, Vol. 3, No. 3, pp. 287-293, 2013.
- [2] E. G. Shehata, Sliding mode direct power control of RSC for DFIGs driven by variable speed wind turbines, *Alexandria Engineering Journal*, Vol. 54, pp. 1067-1075, 2015.

- [3] Y. Wu, W. Yang, Different control strategies on the rotor side converter in DFIG-based wind turbines, *Energy Procedia*, Elsevier, Vol. 100, pp. 551-555, 2016.
- [4] M. Adjoudj, M. Abid, A. Aissaoui, Y. Ramdani, H. Bounoua, Sliding mode control of a double fed induction generator for wind turbines, *Rev. Roum. Sci. Techn. Électrotechn. et Énerg.*, Vol. 56, No. 1, pp. 15-24, 2011.
- [5] H. Benbouhenni, Comparative study between different vector control methods applied to DFIG wind turbines, *Majlesi Journal of Mechatronic Systems*, Vol. 7, No. 4, pp. 15-23, 2018.
- [6] A. Yahdou, B. Hemici, Z. Boudjema, Second order sliding mode control of a dual-rotor wind turbine system by employing a matrix converter, *Journal of Electrical Engineering*, Vol. 16, No. 4, pp. 1-11, 2016.
- [7] Y. Bekakra, D. Ben Attous, Comparison study between SVM and PWM inverter in sliding mode control of active and reactive power control of a DFIG for variable speed wind energy, *International Journal of Renewable Energy Research*, Vol. 2, No. 3, pp. 471-476, 2012.
- [8] Z. Boudjema, A. Meroufel, Y. Djerriri, E. Bounadja, Fuzzy sliding mode control of a doubly fed induction generator for wind energy conversion, *Carpathian Journal of Electronic and Computer Engineering*, Vol. 6, no. 2, pp. 7-14, 2013.
- [9] Z. Boudjema, A. Meroufel, A. Amari, Robust control of a doubly fed induction generator (DFIG) fed by a direct AC-AC converter, *Przełąd Elektrotechniczny*, Vol. 11, pp. 213-221, 2012.
- [10] H. Benbouhenni, Comparative Study between Direct Vector Control and Fuzzy Sliding Mode Controller in Three-Level Space Vector Modulation Inverter of Reactive and Active Power Command of DFIG-Based Wind Turbine Systems, *International Journal Of Smart Grid*, Vol. 2, No. 4, pp. 188-196, 2018.
- [11] H. Benbouhenni, Z. Boudjema, A. Belaidi, Neuro-second order sliding mode control of a DFIG supplied by a two-level NSVM inverter for wind turbine system, *Iranian Journal of Electrical and Electronic Engineering*, Vol. 14, No. 3, 2018, pp.362-373.
- [12] H. Benbouhenni, Z. Boudjema, A. Belaidi, Direct vector control of a DFIG supplied by an intelligent SVM inverter for wind turbine system, *Iranian Journal of Electrical and Electronic Engineering*, Vol. 15, No. 1, pp.45-55, 2019.
- [13] H. Benbouhenni, Z. Boudjema, A. Belaidi, Using three-level Fuzzy space vector modulation method to improve indirect vector control strategy of a DFIG based wind energy conversion systems, *International Journal Of Smart Grid*, Vol. 2, No.3, pp.155-171, 2018.
- [14] H. Benbouhenni, Z. Boudjema, A. Belaidi, DFIG-based wind turbine system using four-level FSVM strategy, *Majlesi Journal of Energy Management*, Vol. 6, No. 3, 2017.
- [15] H. Benbouhenni, Fuzzy second order sliding mode controller based on three-level fuzzy space vector modulation of a DFIG for wind energy conversion systems, *Majlesi Journal of Mechatronic Systems*, Vol. 7, No. 3, pp. 17-26, 2018.
- [16] N. Khemiri, A. Khedher, M. F. Mimouni, Wind energy conversion system using DFIG controlled by backstepping and sliding mode strategies, *International Journal of Renewable Energy Research*, Vol. 2, No. 3, pp. 422-435, 2012.
- [17] Y. Djerriri, A. Meroufel, B. Belabbas, A. Massoum, Three-level NPC voltage source converter based direct power control of the doubly fed induction generator at low constant switching frequency, *Revue des Énergies Renouvelables*, Vol. 16, No. 1, pp. 91-103, 2013.
- [18] Z. Boudjema, R. Taleb, Y. Djerriri, A. Yahdou, A novel direct torque control using second order continuous sliding mode of a doubly fed induction generator for a wind energy conversion system, *Turkish Journal of Electrical Engineering & Computer Sciences*, Vol. 25, pp. 965-975, 2017.
- [19] G. S. Kaloi, J. Wang, M. H. Baloch, Active and reactive power control of the doubly fed induction generator based on wind energy conversion system, *Energy Reports*, Elsevier, Vol. 2, pp. 194-200, 2016.
- [20] M. Benkahla, R. Taleb, Z. Boudjema, Comparative study of robust control strategies for a DFIG-based wind turbine, *International Journal of Advanced Computer Science and Applications*, Vol. 7, No. 2, pp. 455-462, 2016.
- [21] K. Kerrouche, A. Mezouar, Kh. Belkacem, Decoupled control of doubly fed induction generator by vector control for wind energy conversion system, *Energy Procedia*, Elsevier, Vol. 42, pp. 239-248, 2013.
- [22] A. Medjber, A. Moualdia, A. Mellit, M. A. Guessoum, Comparative study between direct and indirect vector control applied to a wind turbine equipped with a double-fed asynchronous machine Article, *International Journal of Renewable Energy Research*, Vol. 3, No. 1, pp. 89-93, 2013.
- [23] H. Benbouhenni, Z. Boudjema, A. Belaidi, Indirect vector control of a DFIG supplied by a two-level FSVM inverter for wind turbine system, *Majlesi Journal of Electrical Engineering*, Vol. 13, No. 1, 2019.
- [24] M. M. Ismail, A. F. Bendary, Protection of DFIG wind turbine using fuzzy logic control, *Alexandria Engineering Journal*, Vol. 55, pp. 941-949, 2016.
- [25] A. Bakouri, H. Mahmoudi, A. Abbou, Intelligent control for doubly fed induction generator connected to the electrical network, *International Journal of Power Electronics and Drive System*, Vol. 7, No. 3, pp. 688-700, 2016.
- [26] B. Belkacem, L. A. Koridak, M. Rahli, Comparative study between SPWM and SVPWM control of a three level voltage inverter dedicated to a variable speed wind turbine, *Journal of Power Technologies*, Vol. 97, No. 3, pp.190-200, 2017.
- [27] A. Kocalims Bilhan, E. Akbal, Modeling and simulation of two-level space vector PWM inverter using photovoltaic cells as DC source, *International Journal of Electronics, Mechanical and Mechatronics Engineering*, Vol. 2, No. 4, pp. 311-317, 2012.
- [28] Z. Boudjema, A. Meroufel, Y. Djerriri, Nonlinear control of a doubly fed induction generator for wind energy conversion, *Carpathian Journal of Electronic and computer Engineering*, Vol. 6, No. 1, pp. 28-35, 2013.
- [29] Z. Boudjema, A. Meroufel, E. Bounadja, Y. Djerriri, Nonlinear control of a doubly fed induction generator supplied by a matrix converter for wind energy conversion systems, *Journal of Electrical Engineering*, Vol. 13, No. 4, pp. 269-276, 2013.
- [30] S. E. Ardjoun, M. Abid, Fuzzy sliding mode control applied to a doubly fed induction generator for wind turbines, *Turkish Journal of Electrical Engineering & Computer Sciences*, Vol. 23, pp. 1673-1686, 2015.
- [31] B. Belabbas, Hybrid fuzzy sliding mode performance control applied to a DFIG system for the production and integrated wind energy into a power grid based three-level converters, *Balkan Journal of Electrical & Computer Engineering*, Vol. 1, No. 2, pp. 93-101, 2013.
- [32] H. Sudheer, SF. Kadad, B. Sarvesh, Improved fuzzy logic based DTC of induction machine for wide range of speed control using AI based controllers, *Journal of Electrical Systems*, Vol. 12, No. 2, pp. 301-314, 2016.
- [33] D. Boudana, L. Nezli, A. Telmcani, M. O. Mahmoudi, M. Tadjine, Robust DTC based on adaptive fuzzy control of double star synchronous machine drive with fixed switching frequency, *Journal of Electrical Engineering*, Vol. 63, No. 3, pp. 133-143, 2012.
- [34] E. Benyoussef, A. Meroufel, S., Barkat, Three-level DTC based on fuzzy logic and neural network of sensorless DSSM using extended kalman filter, *International Journal of Power Electronics and Drive System*, Vol. 5, No. 4, pp. 453-463, 2015.
- [35] H. Benbouhenni, Neuro-second order sliding mode field oriented control for DFIG based wind turbine, *International Journal of Smart Grid*, Vol. 2, No. 4, pp. 209-217, 2018.

Habib Benbouhenni was born in chlef, Algeria. He is a PhD student in the Departement of electrical engineering at the ENPO-MA, Oran, Algeria. He received a M.A. degree in Automatic and informatique industrial in 2017. His research activities include the application of robust control in the wind turbine power systems

Zinelaabidine Boudjema was born in Algeria in 1983. He is Teacher in university of chlef, Algeria. He received a M.S. degree in electrical engineering from ENP of Oran, Algeria in 2010. He received a PhD in Electrical Engineering from university of Sidi Belabes, Algeria 2015. His research activities include the study and application of robust control in the wind-solar power systems.

Abdelkader Belaidi, Professor at the National Polytechnic High School - Maurice Audin in Oran. He obtained his Ph.D in Physics at the University Of East Anglia - UK in 1980. His current fields of interest are Nanotechnology, robotics and Artificial Intelligence.